ACCOUNTS of chemical research

pubs.acs.org/accounts Article

Application of Dislocation Theory to Minimize Defects in Artificial Solids Built with Nanocrystal Building Blocks

Published as part of the Accounts of Chemical Research special issue "Transformative Inorganic Nanocrystals".

Justin C. Ondry and A. Paul Alivisatos*

Cite This: *Acc. Chem. Res.* 2021, 54, 1419−1429 Read Online

ACCESS | Metrics & More | Article Recommendations | Supporting Information

CONSPECTUS: Oriented atomic attachment of colloidal inorganic nanocrystals represents a powerful synthetic method for preparing complex inorganic superstructures. Examples include fusion of nanocrystals into dimer and superlattice structures. If the attachment were perfect throughout, then the resulting materials would have single crystal-like alignment of the individual nanocrystals' atomic lattices. While individual colloidal nanocrystals typically are free of many defects, there are a multitude of pathways that can generate defects upon nanocrystal attachment. These attachment generated defects are typically undesirable, and thus developing strategies to favor defect-free attachment or heal defective interfaces are essential. There may also be some cases where attachment-derived defects are desirable. In this Account, we summarize our current understanding of how these defects arise, in order to offer guidance to those who are designing nanocrystal derived solids.

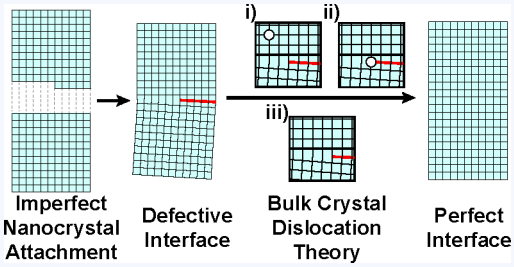

The small size of inorganic nanocrystals means short diffusion lengths to the surface, which favor the formation of nanocrystal building blocks with pristine atomic structures. Upon attachment, however, there are numerous pathways that can lead to atomic scale defects, and bulk crystal dislocation theory provides an invaluable guide to understanding these phenomena. As an example, an atomic step edge can be incorporated into the interface leading to an extra half-plane of atoms, known as an edge dislocation. These dislocations can be well described by the Burgers vector description of dislocations, which geometrically identifies planes in which a dislocation can move. Our *in situ* measurements have verified that bulk dislocation theory predictions for 1D defects hold true at few-nanometer length scales in PbTe and CdSe nanocrystal interfaces. Ultimately, the applicability of dislocation theory to nanocrystal attachment enables the predictive design of attachment to prevent or facilitate healing of defects upon nanocrystal attachment. We applied similar logic to understand formation of planar (2D) defects such as stacking faults upon nanocrystal attachment. Again concepts from bulk crystal defect crystallography can identify attachment pathways that can prevent or deterministically form planar defects upon nanocrystal attachment. The concepts we discuss work well for identifying favorable attachment geometries for nanocrystal *pairs*; however it is currently unclear how to translate these ideas to near-simultaneous multiparticle attachment. Geometric frustration, which prevents nanocrystal rotation, and yet-to-be considered defect generation pathways unique to multiparticle attachment complicate defect-free superlattice attachment. New imaging methods now allow for the direct observation of local attachment trajectories and may enable improved understanding of such multiparticle phenomena. With further refinement, a unified framework for understanding and ultimately eliminating structural defects in fused nanocrystal superstructures may well be achievable in coming years.

KEY REFERENCES

- Ondry, J. C.; Hauwiller, M. R.; Alivisatos, A. P. Dynamics and Removal Pathway of Edge Dislocations in Imperfectly Attached PbTe Nanocrystal Pairs; Towards Design Rules for Oriented Attachment. *ACS Nano* **2018**, *12*, 3178−3189.[1] *In situ TEM studies reveal the importance of dislocation glide plane orientation for facilitating dislocation removal from imperfect interfaces in attached PbTe nanocrystals.*
- Ondry, J. C.; Philbin, J. P.; Lostica, M.; Rabani, E.; Alivisatos, A. P. Resilient Pathways to Atomic Attachment of Quantum Dot Dimers and Artificial Solids from Faceted CdSe Quantum Dot Building Blocks. *ACS Nano* **2019**, *13*, 12322−12344.[2] *Comprehensive in situ TEM studies of dislocation removal pathways in CdSe nanocrystals attached on their prismatic facets.*

Received: November 1, 2020
Published: February 12, 2021

https://dx.doi.org/10.1021/acs.accounts.0c00719
Acc. Chem. Res. 2021, 54, 1419−1429

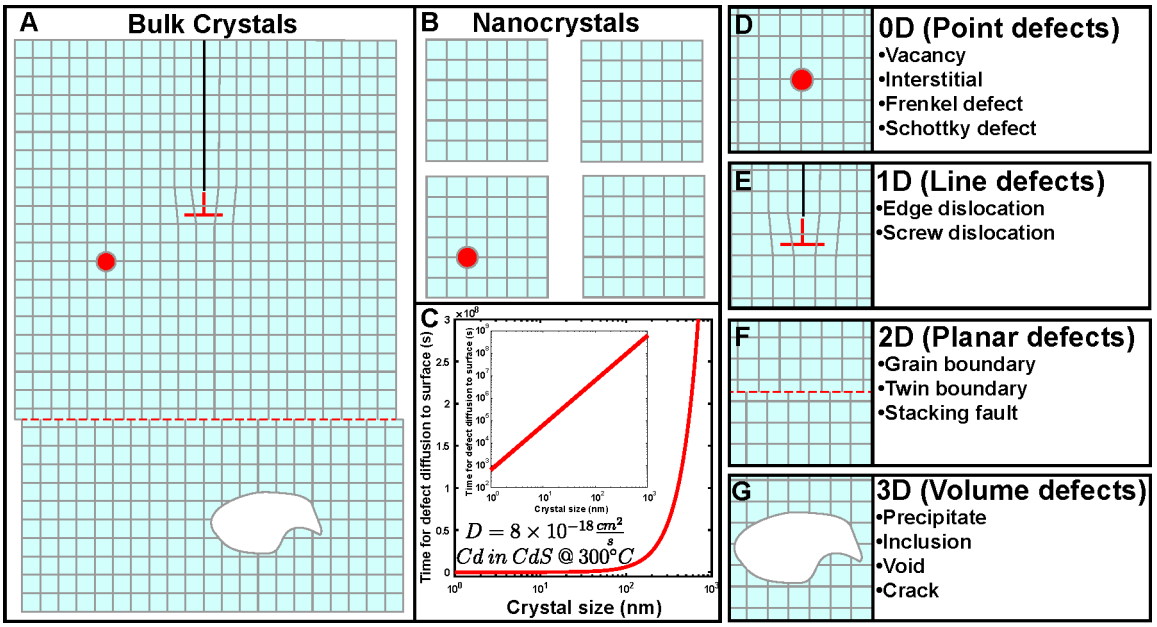

Figure 1. Crystals and their imperfections. (A) Bulk crystal schematic with different structural defect classes, and (B) nanosized crystals, which are typically devoid of nonequilibrium structural defects. (C) Plot of the average time it takes to expel a vacancy in CdS crystallite as a function of crystallite size at 300 °C. The vacancy diffusion coefficient was calculated from Woodbury.[6] (D–G) Classification of structural defects with increasing dimensionality.

1. INTRODUCTION

In the macroworld, properties of matter (density, melting point, refractive index) are intensive quantities, which are independent of system size. At the nanoscale, this relationship breaks down and many materials' properties become strongly system-size dependent. Inorganic colloidal nanocrystals simultaneously display strongly size dependent thermodynamic (e.g., melting point[3] and phase transitions[4]) and electronic properties.[5] As such, understanding the size dependent thermodynamic and kinetic properties related to growth are crucial to engineering size dependent electronic structures. Electronic structure engineering using handles such as size, shape, doping, and composition variation can be used to tailor make structures for various applications (e.g., efficient light emission, charge separation, etc.). As isolated nanocrystals, high-quality samples are routinely achieved. However, for many practical applications nanocrystals must be brought close enough for electronic communication. Atomic attachment of individual nanocrystals enables strong electronic communication between nanocrystals, however challenges need to be overcome to realize high-quality nanocrystal attachment.

In this Account, we will discuss thermodynamic and kinetic factors, which dominate at the nanoscale and favor the formation of defect-free inorganic nanocrystals. Next we will discuss atomically attaching individual nanocrystals into crystallographically fused superstructures. We will focus on attachment mediated defect formation and removal pathways. Our recent *in situ* TEM experiments document defect removal pathways in imperfectly attached PbTe[1] and CdSe[2] pairs and point toward the possibility of a unifying framework to understand and control defects in attached inorganic nanocrystals. Finally we will discuss progress and challenges of translating nanocrystal pair attachment principles to attachment of nanocrystal arrays.

1.1. Imperfections in Crystalline or Nanocrystalline Solids

The small size of colloidal nanocrystals changes kinetic considerations taken for granted in bulk materials. In a bulk crystal (Figure 1A), there are typically imperfections with high energy configurations throughout the volume. Long diffusion distances to surfaces, where these defects can be expelled, make their removal slow and difficult. In contrast, in colloidal nanocrystals (Figure 1B) a free surface is at most a few nanometers away and high energy imperfections can easily be expelled to the surface. In Figure 1C, we consider the size scaling of the time required for a vacancy to diffuse to the surface of CdS crystallites, highlighting the benefit of small crystallites. As a result only defects whose energy are sufficiently low to be present at thermodynamic equilibrium are present (Figure 1B).

To better understand imperfections in crystalline solids, we consider the different classes explicitly. We begin with 0D point defects (Figure 1D), such as vacancies. Vacancies are often considered *equilibrium* defects, since their formation energies are small enough that they exist at equilibrium at finite temperatures. The addition of an extra half-plane of atoms leads to an edge dislocation, which represents a class of 1D defects (Figure 1E). For a 1D defect spanning a crystal, the energy scales with the length and can approach 5 eV/Å, automatically making them nonequilibrium defects.[7] Termination of a lattice plane within a crystal leads to atoms that have dangling bonds and thus typically represent trap states in semiconductors.[8] For 2D planar defects such as grain boundaries (Figure 1F), the energy scales with area, again resulting in large formation energies. Special cases of 2D defects, such as twin boundaries and stacking faults, can have quite low formation energies.[9] Similar, unfavorably high formation energies are present for 3D volume defects (Figure 1G). Typically, 0D defects (Figure 1E) have appreciable thermodynamic concentrations at finite temperatures (k_BT) and all other classes are considered nonequilibrium defects

https://dx.doi.org/10.1021/acs.accounts.0c00719
Acc. Chem. Res. 2021, 54, 1419–1429

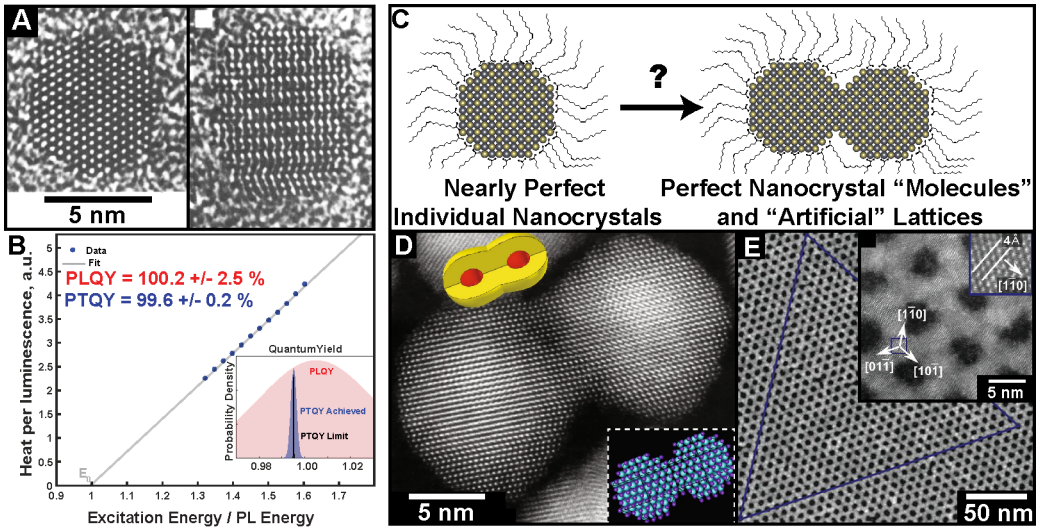

Figure 2. From high-quality individual nanocrystals to attached superstructures. (A) Example of a single crystal wurtzite CdSe nanocrystal. Reproduced with permission from ref 16. Copyright 1995 American Chemical Society. (B) Near-unity quantum yield CdSe/CdS quantum dots. Reproduced with permission from ref 10. Copyright 2019 AAAS. (C) Scheme outlining the challenges converting individual nanocrystals into atomically fused superstructures. (D) Example of an atomically fused CdSe/CdS quantum dot dimer. Reproduced with permission from ref 13. Copyright 2019 Nature Publishing Group. (E) Example honeycomb lattice derived from individual PbSe nanocrystals. Reproduced with permission from ref 14. Copyright 2014 AAAS.

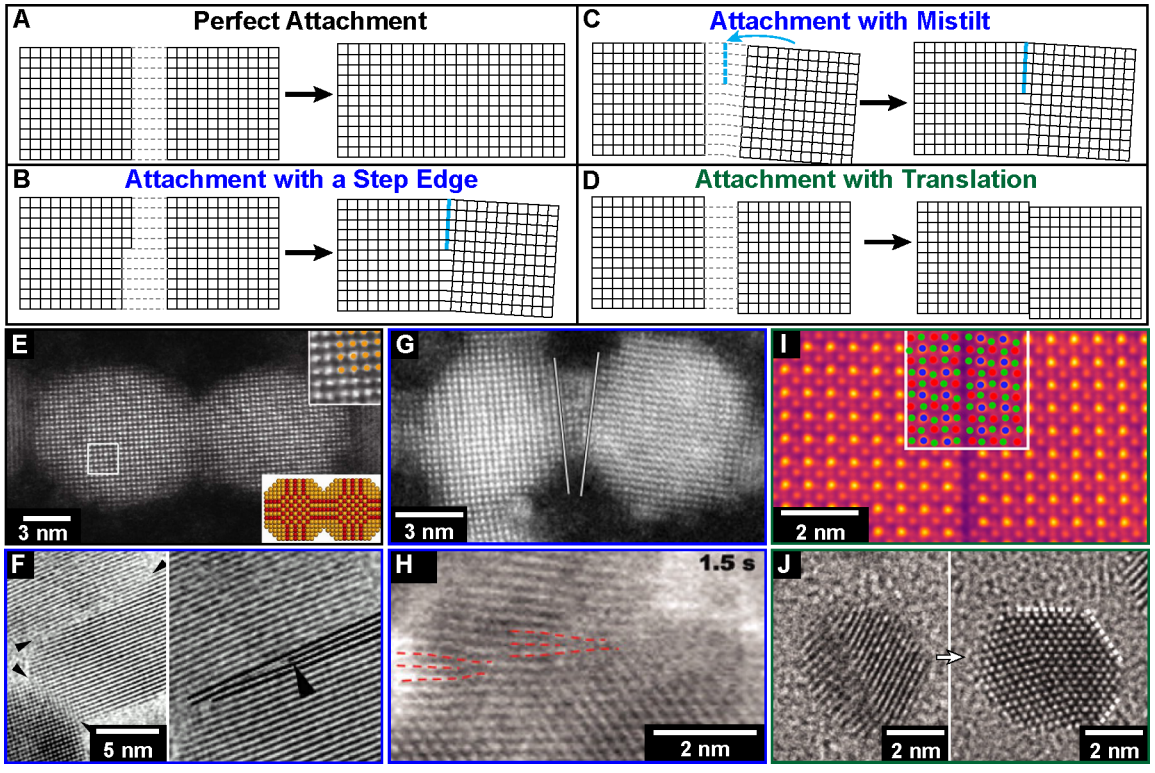

Figure 3. Defect generation pathways during nanocrystal attachment. (A) Perfect attachment, (B) attachment of particles with a step edge, (C) attachment with a mistilt and atomic diffusion into the interface, and (D) attachment with a translation leading to a stacking fault. (E) Example of perfect attachment of PbSe nanocrystals. Reproduced with permission from ref 19. Copyright 2013 American Chemical Society. (F–H) Examples of edge dislocations resulting from nanocrystal attachment in TiO_2, PbSe, and iron oxyhydroxide nanocrystals, respectively. Panel F reproduced with permission from ref 20. Copyright 1998 AAAS. Panel G reproduced with permission from the Supporting Information of ref 19. Copyright 2013 American Chemical Society. Panel H reproduced with permission from ref 17. Copyright 2012 AAAS. Example of stacking fault (I) and twin (J) planar defects resulting from nanocrystal attachment in $CsPbBr_3$ and Pt, respectively. Panel I reproduced with permission from ref 21. Copyright 2018 American Chemical Society. Panel J reproduced with permission from ref 22. Copyright 2012 AAAS.

since they are (typically) kinetically trapped. On these grounds alone, one could anticipate that, based on the facile kinetics of 0D defect removal, it ought to be possible to prepare exceptionally high-quality initial nanocrystal building blocks. On thermodynamic grounds, the high energies of 1D and 2D defects suggest that with the right pathway, it might be possible

https://dx.doi.org/10.1021/acs.accounts.0c00719
Acc. Chem. Res. 2021, 54, 1419–1429

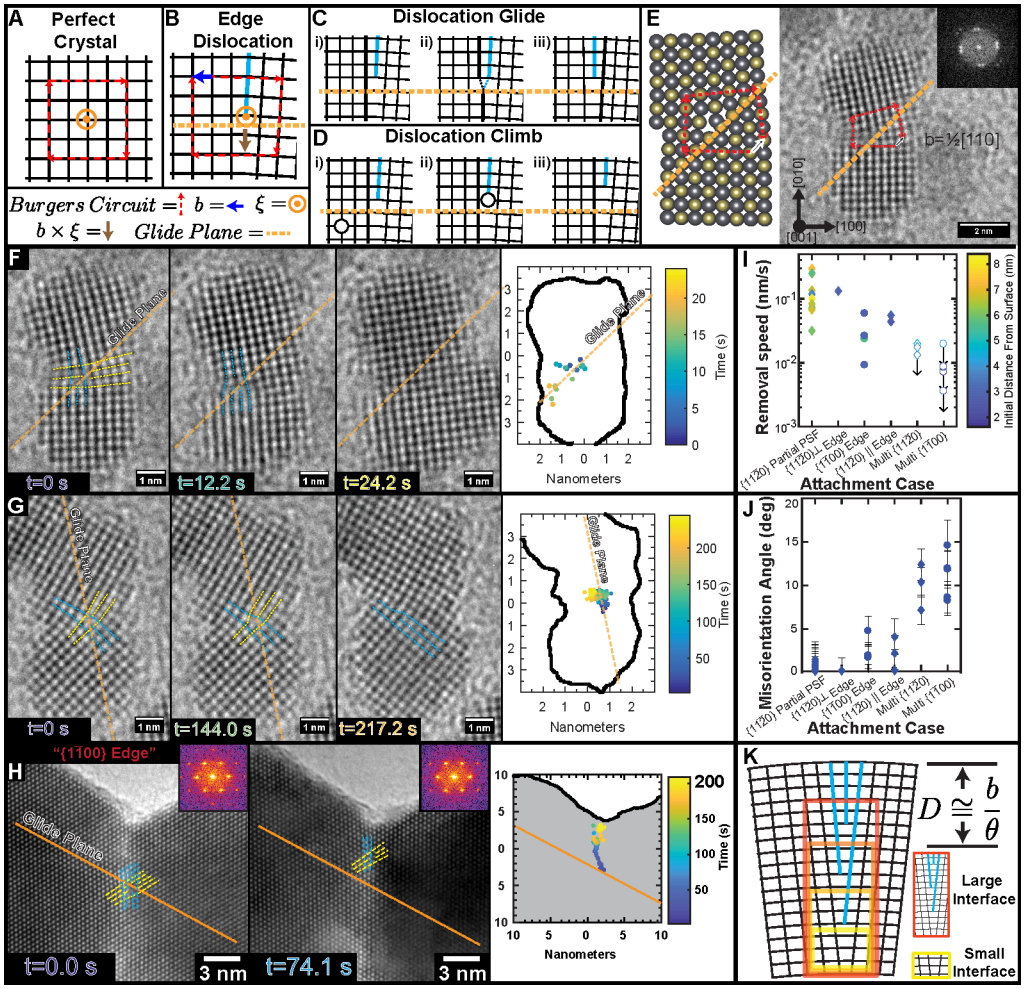

Figure 4. Rational description of edge dislocations in attached nanocrystals. Burgers circuit for (A) a perfect crystal and (B) an edge dislocation. The plane defined by "$\mathbf{b} \times \boldsymbol{\xi}$" is the glide plane (orange dashed line). Mechanism for dislocation (C) glide and (D) climb. (E) Example Burgers circuit for a model (left) and experimental HRTEM image (right) for an imperfect interface in rock salt PbTe with a $\mathbf{b} = \frac{a}{2}\langle 110\rangle$ edge dislocation. (F) Example *in situ* HRTEM trajectory of imperfectly {100} attached PbTe nanocrystals with a $\mathbf{b} = \frac{a}{2}\langle 110\rangle$ dislocation. (G) Example trajectory of imperfectly {110} attached PbTe nanocrystals with a $\mathbf{b} = \frac{a}{2}\langle 110\rangle$ dislocation. Panels E–G reproduced with permission from ref 1. Copyright 2018 American Chemical Society. (H) Example trajectory of imperfectly $\{1\bar{1}00\}$ attached wurtzite CdSe nanocrystals with a $\mathbf{b} = \frac{a}{3}\langle 11\bar{2}0\rangle$ edge dislocation. (I) Classification of dislocation removal speeds and (J) atomic lattice misalignment in imperfectly attached CdSe. (K) Analytic model to predict the number of dislocations for misoriented nanocrystals of a given size. Panels H–K reproduced with permission from ref 2. Copyright 2019 American Chemical Society.

to attach these building blocks into pristine nanocrystal solids. How to think about such pathways is the subject of this Account.

The short diffusion lengths in nanocrystals facilitate removal of nonequilibrium defects. As a result, structurally pristine colloidal nanocrystals can be synthesized at low temperatures compared to bulk melting temperatures. An example of a single crystal wurtzite CdSe nanocrystal is shown in Figure 2A, which is nearly free of structural imperfections (except at stacking fault at the bottom). Through appropriate heterostructure fabrication and surface passivation, CdSe/CdS core–shell semiconductor nanocrystals with luminescence efficiency (quantum yield 99.6% ± 0.2%), which is a proxy for crystal quality, have recently been achieved (Figure 2B).[10] This quantum yield is comparable to MBE and MOCVD grown semiconductor heterostructures. As such, individual colloidal semiconductor nanocrystals are tantalizing building blocks for complex semiconductor assemblies and superlattices.

1.2. Opportunities and Challenges in Nanocrystal Attachment

Atomically fused nanocrystals present exciting opportunities because the all-inorganic interface allows for strong electronic coupling (Figure 2C).[11] Subsequently, this can lead to electronic minibands, which can be engineered in ways atomic bands cannot.[12] However, synthetic pathways for translating individual nanocrystals to pristine attached particles remain unclear. An example of an atomically fused nanocrystal dimer of CdSe/CdS is shown in Figure 2D.[13] Expanding attachment to multiple particles results in, for example, honeycomb lattices of atomically fused PbSe nanocrystals (Figure 2E).[14] Unfortunately many of the predicted properties (such as Dirac minibands[12] and nontrivial flat bands[12]) of these materials remain elusive, likely due to imperfections in the materials.[15]

In this Account, we will consider defect generation upon atomic attachment of individual nanocrystals. We will highlight

https://dx.doi.org/10.1021/acs.accounts.0c00719
Acc. Chem. Res. 2021, 54, 1419–1429

how our recent *in situ* TEM studies of imperfect nanocrystal attachment point to design principles for enhancing defect removal prospects or preventing their formation.[1,2] In section 2, we will discuss sources of imperfections resulting from nanocrystal attachment. In section 3, we will present a dislocation theory framework for rationally describing 1D dislocations in imperfect interfaces. Next in section 4, we will consider 2D planar defects such as stacking faults and present design principles to control or prevent their formation. Finally in section 5, we will consider multiple-nanocrystal attachment and the additional complications that result. We will highlight progress in improving attachment quality and opportunities for additional study regarding atomically fused nanocrystal superlattices. Together we hope this Account provides a road map for mitigating structural imperfections in attached colloidal nanocrystals much like well-established strategies in traditional crystal growth.

2. DEFECT GENERATION FROM NANOCRYSTAL ATTACHMENT

We begin by considering possible configurations for nanocrystal attachment in otherwise pristine nanocrystals. Broadly, to achieve atomic attachment of colloidal nanocrystals, the particles must be oriented with a common crystal alignment. This is typically achieved by rotation of nanocrystals in solution[17] or via shape engineering.[18] First, in Figure 3A, two crystals with atomically flat surfaces can seamlessly join. Experimental examples such as Figure 3E reveal pristine attachment is indeed possible.

Next in Figure 3B, we consider the attachment of two nanocrystals, one of which contains an atomic step on the faceted surface. In this case, the atomic step is incorporated into the interface, leading to the formation of an edge dislocation (1D defect) trapped at the interface. Figure 3F−H show examples of edge dislocations in TiO_2, PbSe, and iron oxyhydroxide, respectively. Alternatively edge dislocations could result from nanocrystals held at a mistilted angle (Figure 3C), and upon attachment, diffusion into the interface incorporates an extra half-plane of atoms.

Another possibility is shown in Figure 3D where two atomically smooth nanocrystals can attach with a fractional unit cell translation, leading to a metastable stacking fault at the interface. Figure 3I shows an example of a stacking fault in attached $CsPbBr_3$ nanocrystals. Analogously, nanocrystals can attach resulting in a twin boundary (Figure 3J). Taken together, Figure 3A−D presents several major pathways that can lead to imperfections upon pristine particle attachment.

3. EDGE DISLOCATIONS

Edge dislocations often result from particle attachment and warrant careful study.[20] We first consider formal definitions of dislocation geometry, which can dictate the directions that a defect can move within a crystal. In the case of a perfect crystal, any closed circuit of translations spanning the same number of atoms returns to the original starting point (Figure 4A). This is known as a Burgers circuit (red dashed line).[23] In the case of an inserted half-plane (light blue), a similar circuit does not return to the starting position (Figure 4B). Instead, the vector needed to close the circuit (dark blue arrow) is defined as the Burgers vector. The line running along the dislocation core is defined as the sense vector, $\boldsymbol{\xi}$ (orange vector perpendicular to the page). Edge dislocations result when $\mathbf{b}$ and $\boldsymbol{\xi}$ are orthogonal, and screw dislocations are the case where $\mathbf{b}$ and $\boldsymbol{\xi}$ are collinear.[7] The plane defined by the cross product of the Burgers vector and sense vector, $\mathbf{b} \times \boldsymbol{\xi}$, (brown arrow) is the glide plane (orange dashed line). This is the plane in which the dislocation can move most easily.[7]

To understand why a dislocation can move easily in its glide plane, we consider Figure 4C where the extra half-plane of atoms can move in the lattice via simple atomic rearrangements at the terminus of the half-plane. Gliding of a dislocation is conservative (i.e., does not require addition or removal of atoms) and is only possible within the glide plane.[7] For movements in directions out of the glide plane, a net flux of atoms is needed. An example of this is shown in Figure 4D where coalescence of a vacancy with the half-plane leads to movement perpendicular to the glide plane ("climb"). Typically dislocation climb is slower than glide since vacancies have a limited concentration.[23]

An example of Burgers vector and glide plane determination in a model and experimental HRTEM image of PbTe nanocrystals imperfectly attached on {100} facets is shown in Figure 4E. section S1 gives a review of the Miller index system. In this case, we observe a $\mathbf{b} = \frac{a}{2}\langle 110\rangle$ edge dislocation indicating the magnitude "$\frac{a}{2}$" and direction "$\langle 110\rangle$" of the Burgers vector. In this case, the glide plane for the dislocation intersects the surface of the attached particles, providing a pathway to the surface. We used *in situ* high resolution TEM at controlled electron beam dose rates (200 kV, 4000 $e^-/(Å^2\ s)$) to simulate thermal annealing and to track the dislocation position (Figure 4F) throughout the trajectory. Indeed the dislocation follows the glide plane to the surface, resulting in a defect free interface after ∼24 s.

We next considered attachment on {110} facets (Figure 4G). We observe the identical dislocation type ($\mathbf{b} = \frac{a}{2}\langle 110\rangle$), but its glide plane is collinear with the attachment direction, resulting in a geometry with no direct glide pathways to the surface. During a total observation time of ∼250 s, the defect does not leave the interface. Based on our results, glide plane orientation relative to the surface dictates dislocation removal kinetics in attached PbTe nanocrystals. This concept may be a powerful tool for identifying attachment facets that may facilitate defect removal, should one form.

Subsequently, we studied wurtzite CdSe nanocrystal attachment on prismatic facets. For wurtzite, we use the Miller−Bravais indexing system (section S1). We observed different classes of defects including edge dislocations, stacking faults, and partial dislocations, due to the complex dislocation landscape in wurtzite.[24,25] Imperfect attachment on $\{1\bar{1}00\}$ facets (Figure 4H) results in an edge dislocation with $\mathbf{b} = \frac{a}{3}\langle 11\bar{2}0\rangle$ Burgers vector. The dislocation glide plane does not provide a pathway to the surface. Interestingly, the interface is successfully healed under simulated annealing in a TEM (200 kV, 5000 $e^-/(Å^2\ s)$) via dislocation climb. Currently, it is unclear why dislocations climb in attached CdSe but not in the PbTe. It is worth noting that Pb atoms require considerably more energy to be displaced by an electron beam compared to Cd, which may account for the apparent differences in these two materials.[26] These results demonstrate that activating dislocation climb enables additional dislocation geometries to be expelled from an imperfect interface.

https://dx.doi.org/10.1021/acs.accounts.0c00719
Acc. Chem. Res. 2021, 54, 1419−1429

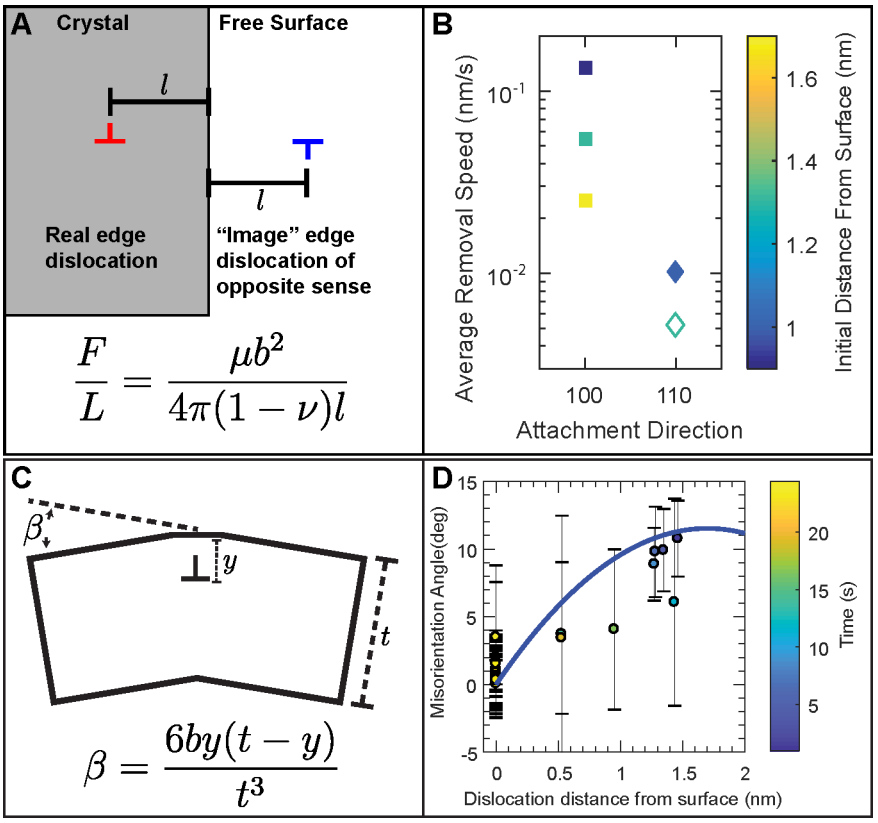

Figure 5. Nanocrystal attachment as a test-bed for nanoscale mechanics. (A) Forces on a dislocation at a free surface where $\frac{F}{L}$ is the force per unit length on the dislocation, μ is the shear modulus, **b** is the Burgers vector, ν is Poisson's ratio, and l is the distance from the surface. (B) Increased removal speed for dislocations that are initially closer to the surface. (C) Continuum mechanics prediction for dislocation induced mistilt, β, as a function of interface thickness, t, dislocation position, y, and Burgers vector, **b**. (D) Experimental mistilt between two PbTe nanocrystals as a function of dislocation position with the analytical result of the equation in panel C plotted in blue. Reproduced with permission from ref 1. Copyright 2018 American Chemical Society.

Several dislocation types were identified in attached CdSe nanocrystals. Through extensive *in situ* TEM experimentation, we identified the relative ease of removal for each defect type (Figure 4I). While the details of these trends are nuanced, overall a larger mistilt of the atomic lattice (Figure 4J) leads to slower defect removal. This suggests that minimizing the angle between particles results in defects that can be more easily removed. This can be understood by considering imperfect nanointerfaces as snapshots of a low angle tilt boundary (Figure 4K) where the dislocation spacing, D, is approximated by $D \approx \frac{\mathbf{b}}{\theta}$. For larger interfaces or larger tilt angles, *two* dislocations are more likely to be incorporated. Multiple dislocations can (attractively) interact via their strain field,[7] hampering removal. In practice, parameters to control relative particle orientation before attachment are unclear. In cases where step edges lead to defects (Figure 3B), developing synthetic methods for step-edge free nanocrystals are needed. Atomic step energies on crystals can vary from 0.01 to 1 eV/Å indicating that surface steps on nanocrystals may have a *thermodynamic* concentration.[27] In cases where forced mistilt from geometric frustration leads to dislocation formation (Figure 3C), self-assembly strategies leading to uniform atomic alignment are needed.

3.1. Dislocation Nanomechanics

Many phenomena of dislocations in bulk materials can be understood using continuum elasticity methods.[7] A defective nanocrystal interface represents a test case for ultrasmall scale defect behaviors. First, we consider the forces acting on a dislocation at a free surface using the image dislocation model (Figure 5A).[7] Continuum elasticity predicts an attractive force the closer the dislocation is to the surface. This would result in defects initially closer to a free surface displaying higher average speed (distance/time) for removal. Indeed Figure 5B qualitatively shows this trend for dislocations in PbTe nanocrystals. Finally, strong surface-attractive forces, which *drive* unstable dislocations out of small crystallites, may be an experimental manifestation of "self-purification"[28−30] in colloidal nanocrystals, which has been largely disproved for 0D dopant atoms, and may be important for removal of other (1D, 2D) structural defects.

Next we consider the mistilt between two particles with a single dislocation at the interface (Figure 5C). The angle (β) between the particles is determined by the interface thickness (t), Burgers vector (**b**), and dislocation position (y) and has been explored for large crystals.[31] At the nanoscale, it predicts that a dislocation leads to large mistilt and successfully predicts the mistilt between PbTe nanocrystals (Figure 5D). Imperfect attachment provides a useful test-bed for single nanometer nanomechanics. At these length scales well-known phenomena are much more dramatic than in larger systems. Future experiments will further our understanding of the mechanical properties of inorganic nanocrystals.

https://dx.doi.org/10.1021/acs.accounts.0c00719
Acc. Chem. Res. 2021, 54, 1419−1429

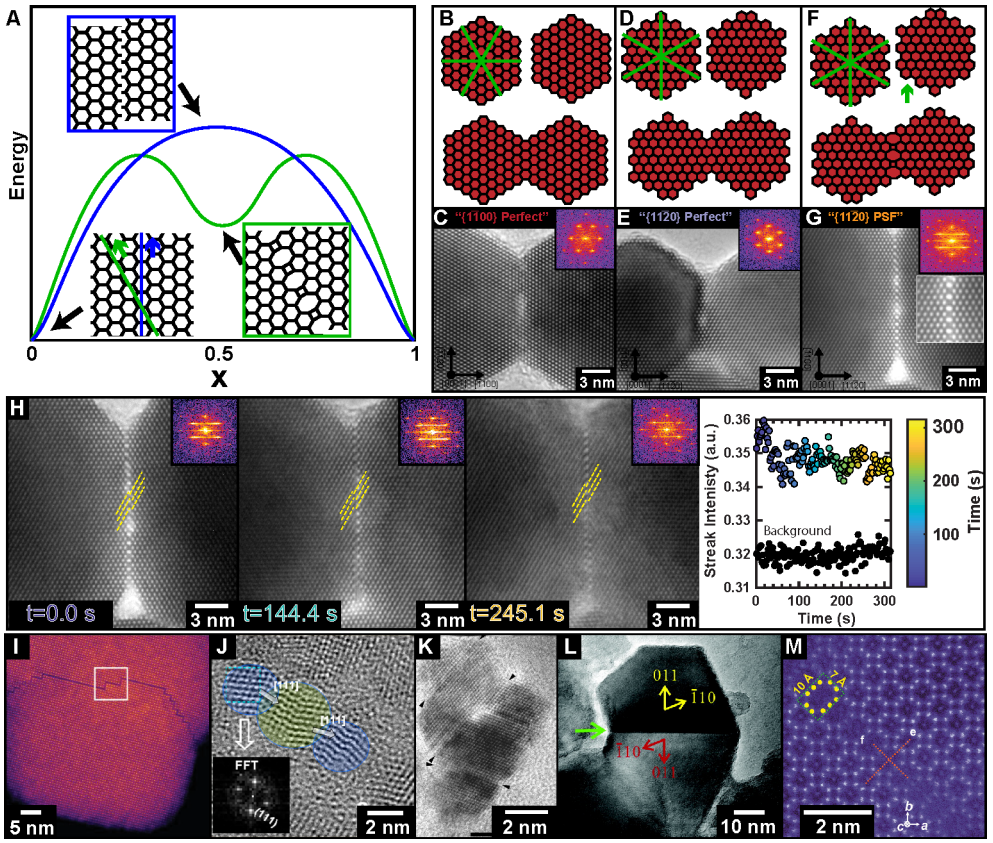

Figure 6. Framework for determining planar defect formation. (A) Relative energy for translating a honeycomb crystal along zig-zag (blue) and armchair planes (green). (B,C) Attachment of wurtzite CdSe on $\{1\bar{1}00\}$ (zigzag) facets allows only perfect attachment. Planes where prismatic stacking faults can form are highlighted in green. (D–G) Attachment of wurtzite CdSe on $\{11\bar{2}0\}$ (armchair) facets has two possibilities, (D, E) perfect attachment and (F, G) formation of a prismatic stacking fault. (H) *In situ* HRTEM showing the stability of a prismatic stacking fault during simulated annealing. Panels C, E, G, and H reproduced with permission from ref 2. Copyright 2019 American Chemical Society. (I) Example of Ruddlesden–Popper defect in perovskite $CsPbBr_3$ nanocrystals attached on {100} facets. Reproduced with permission from ref 32. Copyright 2018 Wiley. (J) Basal plane stacking faults and twins in wurtzite/zinc blende ZnS nanocrystals attached on {0001} facets. Reproduced with permission from ref 33. Copyright 2013 American Chemical Society. (K) Multiple planar defects in attached ZnS. Reproduced with permission from ref 34. Copyright 2003 American Chemical Society. (L) Twin boundary resulting from attachment of TiO_2 nanocrystals on {011} facets. Reproduced with permission from ref 35. Copyright 2004 American Chemical Society. (M) 2 × 3 tunnel defects in α-MnO_2. Reproduced with permission from ref 36. Copyright 2016 American Chemical Society.

4. PLANAR DEFECTS

Unlike dislocations, which have a disrupted local bonding environment at the core of the dislocation, certain planar defects have minimal disruption to the local bonding environment. Thus, certain planar defects are only slightly higher in energy compared to a pristine structure and can be stable minima in the potential energy landscape. We aim to develop design principles to controllably form (or avoid) planar defects resulting from nanocrystal attachment. To illustrate a conceptual framework for identifying attachment geometries that can control planar defect formation, we consider translating part of a honeycomb lattice (Figure 6A) along "zig-zag" and "armchair" planes (blue and green respectively). In zig-zag translations, alternative bonding geometries are not possible, and no metastable energetic minima result. On the other hand, armchair translations of 1/2 unit cell result in a 4–8 membered ring geometry, which is a metastable bonding configuration. This example illustrates the importance of facet geometry in designing defect free interfaces.

Now we consider the case of wurtzite CdSe nanocrystals on their prismatic ($\{1\bar{1}00\}$ and $\{11\bar{2}0\}$) facets. In wurtzite, a $\{11\bar{2}0\}$ prismatic stacking fault is possible and results in a metastable 4–8 membered ring.[37] In the case of attachment on $\{1\bar{1}00\}$ (zig-zag) facets (Figure 6B), the planes that can have a prismatic stacking fault (green) do not coincide with an attachment facet, and as such only the attachment geometry in Figure 6C is observed. In the case of $\{11\bar{2}0\}$ (armchair) attachment, the attachment plane coincides with a plane that can have a prismatic stacking fault. Thus, two possibilities exist: perfect attachment (Figure 6D) or a half unit cell translation leading to a prismatic stacking fault (Figure 6F). Experimentally both perfect (Figure 6E) and prismatic stacking fault (Figure 6G) interfaces are observed for facets. This comparative example illustrates how attachment facet can dictate which planar defects form.

Some planar defects represent metastable structures and thus resist returning to the perfect lattice structure. We observed that a prismatic stacking fault persisted over 300 s of simulated annealing (Figure 6H).[2] This demonstrates the importance of planar defects resulting from attachment since they are difficult to remove. Alternatively this presents an exciting opportunity for planar defect engineering. Some planar defects may harbor useful electronic structures,[38] and

https://dx.doi.org/10.1021/acs.accounts.0c00719
Acc. Chem. Res. 2021, 54, 1419–1429

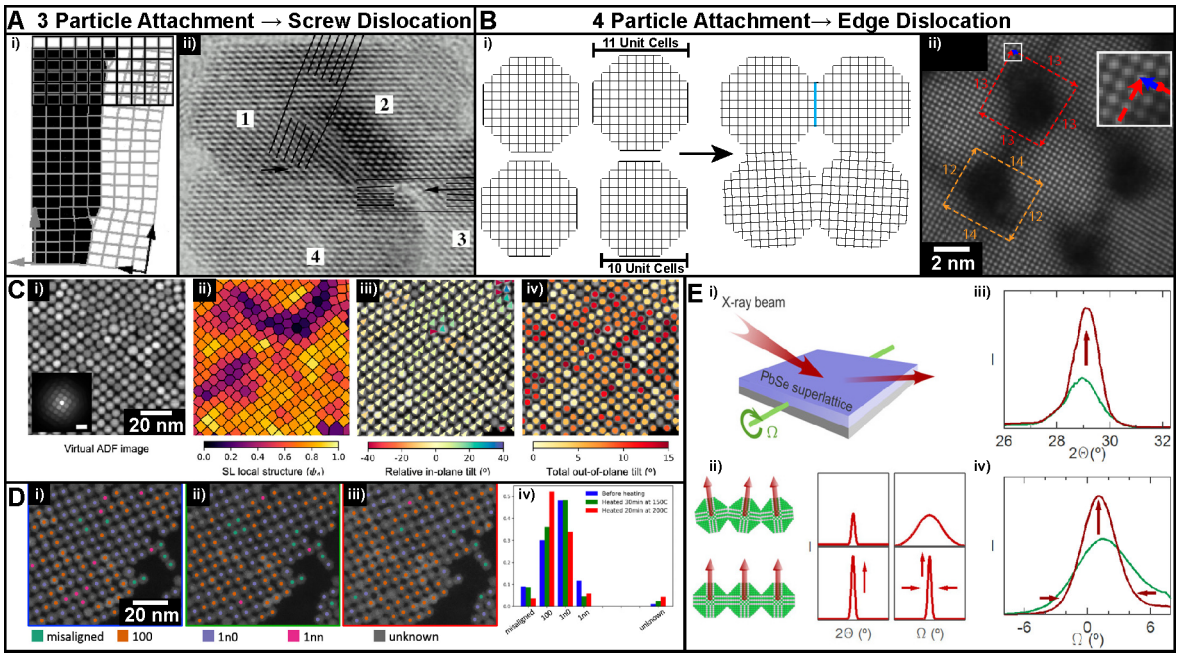

Figure 7. Considerations for multiple particle attachment. (A) Formation of a screw dislocation via 3 particle attachment. Reproduced with permission from ref 20. Copyright 1998 AAAS. (B, i) Attachment of 4 particles with atomically flat facets, but with different sizes leading to a "hollow core" edge dislocation. (B, ii) Experimental example of a hollow core edge dislocation resulting from 4 attached PbSe nanocrystals. Panel B (ii) image reproduced with permission from ref 41. Copyright 2016 American Chemical Society. Burgers circuit annotation added by the current authors. (C) 4D STEM characterization of various order parameters in a PbSe superlattice: (i) virtual dark field image, (ii) local superlattice structure, (iii) in plane tilt of the atomic lattice, and (iv) out of plane tilt of the atomic lattice. Reproduced with permission from ref 42. Copyright 2020 American Chemical Society. (D) Improvement of PbSe nanocrystal alignment upon *in situ* thermal annealing. Reproduced with permission from ref 43. Copyright 2019 Microscopy Society of America. (E) High resolution XRD characterization of PbSe nanocrystal superlattice atomic alignment upon thermal annealing via $2\theta-\Omega$ scans: (i) experimental setup, (ii) effect of orientational alignment diffraction, (iii) experimental 2θ, and (iv) Ω scans. Reproduced with permission from ref 44. Copyright 2019 American Chemical Society.

imperfect (but intentional) attachment may provide a route to high density and possibly even periodic arrangements of such useful imperfections.

Examples of this are already present in the literature. For example in $CsPbBr_3$ and other perovskite crystal structures, Ruddlesden–Popper defects, which lie in {100} planes, are well-known imperfections.[39] Coincidentally, colloidal nanocrystals of $CsPbBr_3$ are usually terminated with {100} facets. Atomic attachment of $CsPbBr_3$ nanocrystals results in Ruddlesden–Popper defects; one such example is shown in Figure 6I. Similarly in the case of attaching wurtzite/zinc blende materials on {0001}/{111} facets, twin boundaries, stacking faults, and coherent phase boundaries can all lie in that plane. Such variety of defects are readily observed, for example, in {0001} attached ZnS nanocrystals (Figure 6J) and in hydrothermally coarsened ZnS (Figure 6K). Additional examples of controlled planar defect formation in TiO_2 and α-MnO_2 are also shown in Figure 6L,M. Ultimately facet specific attachment of colloidal nanocrystals may enable deterministic fabrication of metastable planar defects, which are in and of themselves useful.

5. CONSIDERATIONS FOR MULTIPLE PARTICLE ATTACHMENT

Thus far, we have focused on cases of 2-particle attachment and shown principles from traditional dislocation theory, which explain experimental results in PbTe and CdSe. One of the goals alluded to in Figure 2E is to prepare semiconductor superlattices via attachment of many nanocrystals. For multiple particle attachment, there are additional complications. For example, it has been shown that attachment of a third particle across two already mistilted particles results in the formation of a screw dislocation (Figure 7A).[20] Another possible formation mechanism, which does not need to invoke a step edge, is shown in Figure 7B(i) where one nanocrystal differs in size by a single atomic layer (bottom right). Upon attachment, an extra half-plane is incorporated in the upper interface. This would result in an aptly named "hollow-core" edge dislocation.[40] In Figure 7B(ii), we show an atomic resolution STEM image of attached PbSe nanocrystals collected by Savitzky et al.[41] We overlaid Burgers circuits of a perfect 4 crystal junction (orange) and a hollow core dislocation (red). See Figures S3 and S4 for additional examples in PbSe and CdSe, respectively. The additional complications related to multiparticle attachment create further hurdles in realizing high-quality nanocrystal arrays.

In considering the expansion of few-particle attachment to array attachment, the complexity increases rapidly, and explicitly considering individual attachment events is difficult. In an ideal single crystal, the atomic lattice has one orientation present. Angular mistilts, as we have seen, lead to dislocations and can provide a useful proxy for estimating dislocation density.[45] Local atomic lattice orientation measurements by Dasilva et al. using 4D STEM of attached PbSe nanocrystals have enabled identification of the 3D atomic lattice orientation (Figure 7C(iii,iv)). These measurements coupled with measurements of superlattice order parameters (ψ_4) (Figure 7C(i,ii)) provide a detailed understanding of the coupled atomic and mesoscale order. The ultimate goal is to identify the assembly and attachment conditions and postprocessing leading to each

https://dx.doi.org/10.1021/acs.accounts.0c00719
Acc. Chem. Res. 2021, 54, 1419–1429

nanocrystal achieving the same atomic lattice orientation. Toward that goal, Smeaton et al. performed *in situ* annealing on a superlattice of attached PbSe nanocrystals (Figure 7D).[43] Measurement of the out of plane tilt of individual nanocrystals shows that thermal annealing increases the uniformity in a small field of view. To probe the improved atomic alignment on larger length scales, Walravens et al. used $2\theta-\Omega$ XRD scans to highlight improved atomic alignment across large area films upon thermal annealing (Figure 7E).[44]

Careful atomic lattice orientation mapping presented in Figure 7C highlights the considerable variability in attached semiconductor superlattices, and the implicit lower crystal quality due to tilt induced dislocations and strain. As such, developing strategies for improving alignment of particles during assembly or attachment or postsynthetically represent open research directions, and the work of Dasilva et al.[42] presents a powerful characterization framework. Further, the work of Smeaton et al.[43] and Walravens et al.[44] illustrates that thermal annealing does improve atomic alignment; however even in their samples, annealing does not yet result in uniform atomic alignment within the samples. Recent reports of 3D nanocrystal superlattice attachment[46] highlight the versatility of these strategies; however 3D assemblies likely suffer from geometric frustration like 2D superlattices. Refinement of nanocrystal synthesis or improvement of initial assembly and attachment uniformity may be needed.

6. CONCLUSION AND PERSPECTIVES

In this Account we have outlined the framework for considering defects in colloidal inorganic semiconductor nanocrystals. Kinetic factors which are only apparent in nanoscale crystals greatly facilitate defect-free synthesis of nanocrystals. Atomic attachment of nanocrystals leads to many exciting possibilities; however it is also a potent generator of 1D and 2D crystal defects. We demonstrated how dislocation theory and the Burgers vector notation are powerful tools for predicting 1D defect behavior and provide a design principle to identify facets that provide defects with a path to the surface. We further demonstrated how attachment facet choice can control planar (2D) defect formation, a useful design principle to avoid defects or controllably introduce them into crystals. Finally we highlighted recent progress and challenges understanding attachment and defect generation in multiparticle nanocrystal attachment and atomically fused nanocrystal superlattices.

We take a moment to consider the merits and challenges for attaching nanocrystals into dimer structures and superlattice structures. For a dimer, the nanocrystals can rotate freely, allowing perfect atomic alignment. Superlattices are geometrically frustrated, and nanocrystal rotation can be impinged by neighboring nanocrystals, preventing collective alignment. The degree of crystal misalignment (3°−15°) in attached quantum dot superlattices is much larger than that in epitaxial growth mechanisms (≪1°). Ultimately the mistilt between nanocrystals is a source of crystal defects and strain. These challenges indicate that it may be possible to achieve pristine materials in dimer structures but the path is less certain for arrays.

The atomic lattice is the strongest perturbation an electron (or hole) feels, and thus defects in the atomic lattice will strongly affect carriers. Smaller perturbations from mesoscale superlattices may be drowned out by atomic scale defects. Future endeavors to understand improvements to nanocrystal assembly and attachment should consider fundamental limits for perfection (i.e., dislocation density, positional order, etc.) and importantly whether those limits will be sufficient for engineered miniband structures or other emergent phenomena. We hope the dislocation theory framework for understanding the behavior of defective nanocrystal attachment interfaces outlined here will help identify routes to improve crystal quality in attached nanocrystals. Finally we suggest that nanocrystal attachment may provide a useful synthetic route to desirable planar defects, and thus high defect densities from attachment are a benefit.

■ ASSOCIATED CONTENT

Supporting Information

The Supporting Information is available free of charge at https://pubs.acs.org/doi/10.1021/acs.accounts.0c00719.

Miller and Miller−Bravais indices and dislocations from multiparticle attachment (PDF)

■ AUTHOR INFORMATION

Corresponding Author

A. Paul Alivisatos − *Department of Chemistry and Department of Materials Science and Engineering, University of California, Berkeley, California 94720, United States; Kavli Energy NanoScience Institute, Berkeley, California 94720, United States; Materials Sciences Division, Lawrence Berkeley National Laboratory, Berkeley, California 94720, United States;* orcid.org/0000-0001-6895-9048; Email: paul.alivisatos@berkeley.edu

Author

Justin C. Ondry − *Department of Chemistry, University of California, Berkeley, California 94720, United States; Kavli Energy NanoScience Institute, Berkeley, California 94720, United States;* orcid.org/0000-0001-9113-3420

Complete contact information is available at: https://pubs.acs.org/10.1021/acs.accounts.0c00719

Notes

The authors declare no competing financial interest.

Biographies

Justin Ondry received his B.S. in chemistry/materials science from the University of California, Los Angeles, in 2015 where he performed undergraduate research with Prof. Sarah H. Tolbert. He received his Ph.D. in physical chemistry (Advisor, A. Paul Alivisatos) from the University of California, Berkeley, in 2020. He primarily studied dislocations and their dynamics in imperfectly attached colloidal nanocrystals using *in situ* transmission electron microscopy.

A. Paul Alivisatos is the Samsung Distinguished Professor of Nanoscience and Nanotechnology and a Professor of Chemistry and Materials Science & Engineering at the University of California, Berkeley. Contributions to the fundamental physical chemistry of nanocrystals are the hallmarks of his research group. He was the founding editor of *Nano Letters*, a leading scientific publication of the American Chemical Society in nanoscience.

■ ACKNOWLEDGMENTS

This work was supported by the National Science Foundation, Division of Materials Research (DMR), under Award Number DMR-1808151 and by the U.S. Department of Energy, Office

of Science, Office of Basic Energy Sciences, Materials Sciences and Engineering Division, under Contract No. DE- AC02-05-CH11231, within the Physical Chemistry of Inorganic Nanostructures Program (KC3103). J.C.O. gratefully acknowledges the support of the Kavli Philomathia Graduate Student Fellowship. The authors thank Michelle Crook, Jakob Dahl, and Amy McKeown-Green for critical review of the manuscript.

REFERENCES

(1) Ondry, J. C.; Hauwiller, M. R.; Alivisatos, A. P. Dynamics and Removal Pathway of Edge Dislocations in Imperfectly Attached PbTe Nanocrystal Pairs; Towards Design Rules for Oriented Attachment. *ACS Nano* **2018**, *12*, 3178−3189.
(2) Ondry, J. C.; Philbin, J. P.; Lostica, M.; Rabani, E.; Alivisatos, A. P. Resilient Pathways to Atomic Attachment of Quantum Dot Dimers and Artificial Solids from Faceted CdSe Quantum Dot Building Blocks. *ACS Nano* **2019**, *13*, 12322−12344.
(3) Goldstein, A. N.; Echer, C. M.; Alivisatos, A. P. Melting in semiconductor nanocrystals. *Science* **1992**, *256*, 1425−7.
(4) Tolbert, S. H.; Alivisatos, a. P. Size Dependence of a First Order Solid-Solid Phase Transition: The Wurtzite to Rock Salt Transformation in CdSe Nanocrystals. *Science* **1994**, *265*, 373−6.
(5) Efros, A. L.; Rosen, M. The Electronic Structure of Semiconductor Nanocrystals. *Annu. Rev. Mater. Sci.* **2000**, *30*, 475−521.
(6) Woodbury, H. H. Diffusion of Cd in CdS. *Phys. Rev.* **1964**, *134*, A492−A498.
(7) Anderson, P. M.; Hirth, J. P.; Lothe, J. *Theory of Dislocations*, 3rd ed.; Cambridge University Press, 2017.
(8) Queisser, H. J.; Haller, E. E. Defects in Semiconductors: Some Fatal, Some Vital. *Science* **1998**, *281*, 945−950.
(9) Takeuchi, S.; Suzuki, K.; Maeda, K.; Iwanaga, H. Stacking-fault energy of II-VI compounds. *Philos. Mag. A* **1985**, *50*, 171−178.
(10) Hanifi, D. A.; Bronstein, N. D.; Koscher, B. A.; Nett, Z.; Swabeck, J. K.; Takano, K.; Schwartzberg, A. M.; Maserati, L.; Vandewal, K.; van de Burgt, Y.; Salleo, A.; Alivisatos, A. P. Redefining near-unity luminescence in quantum dots with photothermal threshold quantum yield. *Science* **2019**, *363*, 1199−1202.
(11) Baumgardner, W. J.; Whitham, K.; Hanrath, T. Confined-but-connected quantum solids via controlled ligand displacement. *Nano Lett.* **2013**, *13*, 3225−3231.
(12) Kalesaki, E.; Delerue, C.; Morais Smith, C.; Beugeling, W.; Allan, G.; Vanmaekelbergh, D. Dirac cones, topological edge states, and nontrivial flat bands in two-dimensional semiconductors with a honeycomb nanogeometry. *Phys. Rev. X* **2014**, *4*, 011010.
(13) Cui, J.; Panfil, Y. E.; Koley, S.; Shamalia, D.; Waiskopf, N.; Remennik, S.; Popov, I.; Oded, M.; Banin, U. Colloidal quantum dot molecules manifesting quantum coupling at room temperature. *Nat. Commun.* **2019**, *10*, 5401.
(14) Boneschanscher, M.; Evers, W. H.; Geuchies, J. J.; Altantzis, T.; Goris, B.; Rabouw, F.; van Rossum, S. A. P.; van der Zant, H. S. J.; Siebbeles, L. D. A.; Van Tendeloo, G.; Swart, I.; Hilhorst, J.; Petukhov, A.; Bals, S.; Vanmaekelbergh, D. Long-range orientation and atomic attachment of nanocrystals in 2D honeycomb superlattices. *Science* **2014**, *344*, 1377−1380.
(15) Whitham, K.; Yang, J.; Savitzky, B. H.; Kourkoutis, L. F.; Wise, F.; Hanrath, T. Charge transport and localization in atomically coherent quantum dot solids. *Nat. Mater.* **2016**, *15*, 557−563.
(16) Shiang, J. J.; Kadavanich, A. V.; Grubbs, R. K.; Alivisatos, A. P. Symmetry of annealed wurtzite CdSe nanocrystals. Assignment to C3vpoint group. *J. Phys. Chem.* **1995**, *99*, 17417−17422.
(17) Li, D.; Nielsen, M.; Lee, J.; Frandsen, C.; Banfield, J. F.; De Yoreo, J. J. Direction-Specific Interactions Control Crystal Growth by Oriented Attachment. *Science* **2012**, *336*, 1014−1018.
(18) Van Der Stam, W.; Rabouw, F. T.; Vonk, S. J.; Geuchies, J. J.; Ligthart, H.; Petukhov, A. V.; De Mello Donega, C. Oleic Acid-Induced Atomic Alignment of ZnS Polyhedral Nanocrystals. *Nano Lett.* **2016**, *16*, 2608−2614.
(19) Evers, W. H.; Goris, B.; Bals, S.; Casavola, M.; De Graaf, J.; van Roij, R.; Dijkstra, M.; Vanmaekelbergh, D. Low-dimensional semiconductor superlattices formed by geometric control over nanocrystal attachment. *Nano Lett.* **2013**, *13*, 2317−2323.
(20) Penn, R. L.; Banfield, J. Imperfect Oriented Attachment: Dislocation Generation in Defect-Free Nanocrystals. *Science* **1998**, *281*, 969−971.
(21) Morrell, M. V.; He, X.; Luo, G.; Thind, A. S.; White, T. A.; Hachtel, A.; Borisevich, A. Y.; Idrobo, J.-c.; Mishra, R.; Xing, Y. Significantly Enhanced Emission Stability of CsPbBr3 Nanocrystals via Chemically Induced Fusion Growth for Optoelectronic Devices via Chemically Induced Fusion Growth for Optoelectronic Devices. *ACS Applied Nano Materials* **2018**, *1*, 6091−6098.
(22) Yuk, J. M.; Park, J.; Ercius, P.; Kim, K.; Hellebusch, D. J.; Crommie, M. F.; Lee, J. Y.; Zettl, A.; Alivisatos, A. P. High-Resolution EM of Colloidal Nanocrystal Growth Using Graphene Liquid Cells. *Science* **2012**, *336*, 61−64.
(23) Cai, W.; Nix, W. D. *Imperfections in Crystalline Solids*; Cambridge University Press, 2016.
(24) Osipiyan, Y. A.; Smirnova, I. S. Perfect Dislocations in the Wurtzite Lattice. *Phys. Status Solidi B* **1968**, *30*, 19−29.
(25) Osipyan, Y. A.; Smirnova, I. S. Partial dislocations in the wurtzite lattice. *J. Phys. Chem. Solids* **1971**, *32*, 1521−1530.
(26) Egerton, R.; Li, P.; Malac, M. Radiation damage in the TEM and SEM. *Micron* **2004**, *35*, 399−409.
(27) Jeong, H.-C.; Williams, E. D. Steps on surfaces: experiment and theory. *Surf. Sci. Rep.* **1999**, *34*, 171−294.
(28) Dalpian, G.; Chelikowsky, J. Self-Purification in Semiconductor Nanocrystals. *Phys. Rev. Lett.* **2006**, *96*, 226802.
(29) Du, M. H.; Erwin, S. C.; Efros, A. L.; Norris, D. J. Comment on "self-purification in semiconductor nanocrystals. *Phys. Rev. Lett.* **2008**, *100*, 179702.
(30) Dalpian, G. M.; Chelikowsky, J. R. Dalpian and Chelikowsky reply: *Phys. Rev. Lett.* **2008**, *100*, 179703.
(31) Siems, R.; Delavignette, P.; Amelinckx, S. The buckling of a thin plate due to the presence of an edge dislocation. *Phys. Status Solidi B* **1962**, *2*, 421−438.
(32) Thind, A. S.; Luo, G.; Hachtel, J. A.; Morrell, M. V.; Cho, S. B.; Borisevich, A. Y.; Idrobo, J.-C.; Xing, Y.; Mishra, R. Atomic Structure and Electrical Activity of Grain Boundaries and Ruddlesden-Popper Faults in Cesium Lead Bromide Perovskite. *Adv. Mater.* **2019**, *31*, 1805047.
(33) Sarkar, S.; Acharya, S.; Chakraborty, A.; Pradhan, N. Zinc blende 0D quantum dots to wurtzite 1D quantum wires: The oriented attachment and phase change in ZnSe nanostructures. *J. Phys. Chem. Lett.* **2013**, *4*, 3292−3297.
(34) Huang, F.; Zhang, H.; Banfield, J. F. Two-stage crystal-growth kinetics observed during hydrothermal coarsening of nanocrystalline ZnS. *Nano Lett.* **2003**, *3*, 373−378.
(35) Tsai, M. H.; Chen, S. Y.; Shen, P. Imperfect oriented attachment: Accretion and defect generation of nanosize rutile condensates. *Nano Lett.* **2004**, *4*, 1197−1201.
(36) Yuan, Y.; Wood, S. M.; He, K.; Yao, W.; Tompsett, D.; Lu, J.; Nie, A.; Islam, M. S.; Shahbazian-Yassar, R. Atomistic insights into the oriented attachment of tunnel-based oxide nanostructures. *ACS Nano* **2016**, *10*, 539−548.
(37) Vermaut, P.; Nouet, G.; Ruterana, P. Observation of two atomic configurations for the 1120 stacking fault in wurtzite (Ga, Al) nitrides. *Appl. Phys. Lett.* **1999**, *74*, 694−696.
(38) Dick, K. A.; Thelander, C.; Samuelson, L.; Caroff, P. Crystal phase engineering in single InAs nanowires. *Nano Lett.* **2010**, *10*, 3494−3499.
(39) Ruddlesden, S. N.; Popper, P. The compound Sr 3 Ti 2 O 7 and its structure. *Acta Crystallogr.* **1958**, *11*, 54−55.
(40) Qian, W.; Rohrer, G. S.; Skowronski, M.; Doverspike, K.; Rowland, L. B.; Gaskill, D. K. Open-core screw dislocations in GaN epilayers observed by scanning force microscopy and high-resolution transmission electron microscopy. *Appl. Phys. Lett.* **1995**, *67*, 2284.

https://dx.doi.org/10.1021/acs.accounts.0c00719
Acc. Chem. Res. 2021, 54, 1419−1429

(41) Savitzky, B. H.; Hovden, R.; Whitham, K.; Yang, J.; Wise, F.; Hanrath, T.; Kourkoutis, L. F. Propagation of Structural Disorder in Epitaxially Connected Quantum Dot Solids from Atomic to Micron Scale. *Nano Lett.* **2016**, *16*, 5714−5718.
(42) Dasilva, J. C.; Smeaton, M. A.; Dunbar, T. A.; Xu, Y.; Balazs, D. M.; Kourkoutis, L. F.; Hanrath, T. Mechanistic Insights into Superlattice Transformation at a Single Nanocrystal Level Using Nanobeam Electron Diffraction. *Nano Lett.* **2020**, *20*, 5267−5274.
(43) Smeaton, M. A.; Balazs, D. M.; Hanrath, T.; Kourkoutis, L. F. Quantifying Atomic-Scale Quantum Dot Superlattice Behavior Upon in situ Heating. *Microsc. Microanal.* **2019**, *25*, 1538−1539.
(44) Walravens, W.; Solano, E.; Geenen, F.; Dendooven, J.; Gorobtsov, O.; Tadjine, A.; Mahmoud, N.; Ding, P. P.; Ruff, J. P.; Singer, A.; Roelkens, G.; Delerue, C.; Detavernier, C.; Hens, Z. Setting Carriers Free: Healing Faulty Interfaces Promotes Delocalization and Transport in Nanocrystal Solids. *ACS Nano* **2019**, *13*, 12774−12786.
(45) Kopp, V. S.; Kaganer, V. M.; Baidakova, M. V.; Lundin, W. V.; Nikolaev, A. E.; Verkhovtceva, E. V.; Yagovkina, M. A.; Cherkashin, N. X-ray determination of threading dislocation densities in GaN/Al2O3(0001) films grown by metalorganic vapor phase epitaxy. *J. Appl. Phys.* **2014**, *115*, 073507.
(46) Abelson, A.; Qian, C.; Salk, T.; Luan, Z.; Fu, K.; Zheng, J.-G.; Wardini, J. L.; Law, M. Collective topo-epitaxy in the self-assembly of a 3D quantum dot superlattice. *Nat. Mater.* **2020**, *19*, 49−55.

https://dx.doi.org/10.1021/acs.accounts.0c00719
Acc. Chem. Res. 2021, 54, 1419−1429